Multi-pixel X-ray detection integrated at the end of a narrow multicore fiber

CARLOS CHACON[1], MIGUEL SUAREZ[1], VAHE KARAKHANYAN[1], KEWIN DESJARDIN[2], CLAUDE MENNEGLIER[2], OLIVIER SOPPERA[3,4], VIRGINIE MOUTARLIER[5], AND THIERRY GROSJEAN[*,2]

[1] *University of Franche-Comte, FEMTO-ST Institute, CNRS, UMR 6174, Besançon, France*
[2] *Synchrotron SOLEIL, Saint-Aubin, 9aint-Aubin, 91192 Gif-sur-Yvette, France*
[3] *Université de Haute-Alsace, CNRS, IS2M UMR 7361, F-68100 Mulhouse, France*
[4] *Université de Strasbourg, 67000 Strasbourg, France*
[5] *UTINAM Institute - CNRS UMR 6213 - University of Bourgogne Franche-Comte, Besançon, France*
[*] *Corresponding author: thierry.grosjean@univ-fcomte.fr*

Compiled November 9, 2023

We introduce and demonstrate the concept of a multi-pixel detector integrated at the tip of an individual multicore fiber. A pixel consists here of an aluminum-coated polymer microtip incorporating a scintillating powder. Upon irradiation, the luminescence released by the scintillators is efficiently transferred into the fiber cores owing to the specifically elongated metal-coated tips which ensure efficient luminescence matching to the fiber modes. Each pixel being selectively coupled to one of the cores of the multicore optical fiber, the resulting fiber-integrated X-ray detection process is totally free from inter-pixel cross-talk. Our approach holds promise for fiber-integrated probes and cameras for remote X- and Gamma-ray analysis and imaging in hard-to-reach environments.

http://dx.doi.org/10.1364/ao.XX.XXXXXX

The need for novel tools able to detect ionizing radiations within tiny recesses and/or extreme environments (of high pressure, temperature or radioactivity) is seen to rapidly grow in many scientific, medical and industrial domains. Being compact, robust and flexible, optical fibers are widely considered as a promising optical tool for addressing this demand, as they allow a direct control on light encoded information collected from hard-to-reach locations.

Fiber probes based on the integration of a scintillating element onto the tip of the optical fiber have been widely explored for the local and real-time dosimetry of ionizing radiations. Given their inert, passive, and possibly biocompatible nature, such devices are particularly appealing in a variety of applications and techniques ranging from in-vivo dosimetry in cancer therapies to *in situ* dosimetry within harsh environments such as a nuclear reactor [1–5]. Reaching such a degree of miniaturization from a direct X-ray-to-electron conversion within microfabricated silicon[6], diamond[7] or perovskite [8] structures remains a challenge. Note however that perovskite materials provide a new generation of scintillators of unmatched properties, thus opening new prospects in the design of indirect detection of X-rays [9].

Most of fiber-integrated X-ray detector consist of single pixel systems obtained by coupling a scintillating micro-cell to an individual fiber. Bringing multi-pixel X-ray detectors within hard-to-reach environments would enable new opportunities in radiation analysis, opening the prospect of *in vivo* or *in situ* real-time imaging. However, integrating a pixel array in a compact fiber-integrated architecture remains a challenge. The parallel implementation of a single pixel fiber probe in a fiber bundle represents limits in terms of compactness and image sampling [10] since optical fibers are usually larger than 90 μm (outer diameter including protective coating).

Compactness and resolution issues can be alleviated by implementing multiple pixels onto the same optical fiber. Linares et al. developed a three-pixel detector integrated at the end of an individual fiber that is sufficiently compact to be inserted within a catheter (for brachytherapy monitoring) [11]. However, since the luminescence spectra of the three different scintillators used as detection pixels noticeably overlap, the detector suffers from inter-pixel cross-talk. The development of an array of detection pixels at the tip of an individual optical fiber has so far never been reported.

In this paper, we demonstrate a seven-pixel X-ray detection platform engineered at the tip of an individual fiber. Our detector is achieved by coupling seven metal-coated scintillating micro-tips to a multicore fiber, each microtip being coupled to one of the fiber cores. The resulting seven parallel detection channels are shown to be totally independent from each other, thus holding promise for a high contrast real-time imaging in hard-to-reach environment. Multicore fibers have recently demonstrated new prospects for sensing applications [12, 13] and lab-on-fiber technology [14, 15] with recent important achievements in optical detection [16, 17]. We here extend the multicore-fiber-based technology to the analysis and imaging via ionizing radiations.

Our fiber-integrated multipixel detection system is fabricated using a photopolymerization process at one endface of a 1.5-meter multicore fiber from Fibercore (Model SM-7C1500). The optical fiber shows seven 6.3-μm-diameter cores arranged in a hexagonal lattice, with a 35-μm inter-core spacing. The photopolymerization process involves a scintillating photopolymer locally exposed to a laser light travelling through the fiber. One fiber endface is immersed within the polymer/scintillator mixture while an expanded laser beam (λ=521 nm, laser diode from Thorlabs) is projected onto the other end to homogeneously illuminate all the seven cores of the fiber. The so-excited seven parallel fiber modes carry almost the same power, thereby similarly triggering polymer hardening at the core outputs. The total laser power at the fiber output and exposure time are 0.7 μW and 4 seconds, respectively. After fiber rinsing with ethanol, seven scintillating microtips arranged in a hexagonal lattice appear at the fiber output face. Being realized from the fiber modes themselves at a wavelength closely approaching that of the scintillator luminescence, the so-produced elongated scintillating microtips are expected to reciprocally efficiently transfer their X-ray excited luminescence into the fiber [18]. To increase probe efficiency, the multipixel detection array can be metal coated to limit the luminescence leaving the microtips outside the fiber. Metal coating involves here the deposition of a few-nanometer-thick titanium adhesion layer followed by a 125-nm thick aluminum layer. Aluminum is chosen for its high reflectivity at visible wavelengths and high transparency to X-rays. Note that polymer growth at the endface of a multicore fiber has been reported by Dika et al. [19].

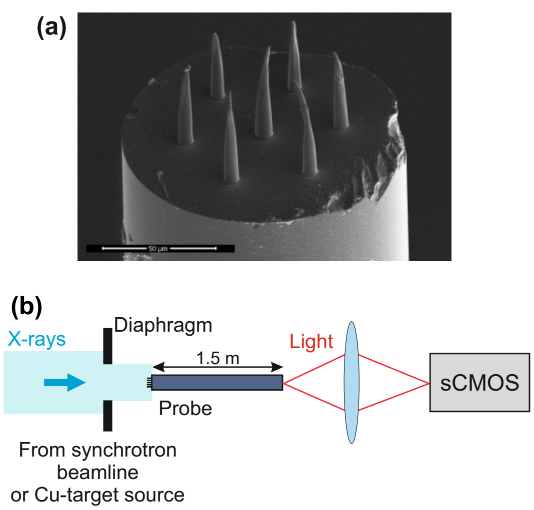

Fig. 1. (a) SEM image of a fiber-integrated multi-pixel detection array on top of a seven-core optical fiber. Each pixel is in direct optical coupling with one of the fiber core. (b) Scheme of the experimental set-up for the detector demonstration.

To produce the scintillating photopolymer, we first grind a commercial Gd_2O_2S:Eu powder (Phosphor Technology, Ref.UKL63/UF-R1) in a mortar with a pestle. The ground powder is then mixed with ethanol to be filtered with a cellulose acetate membrane whose pore diameter is of 1.2 μm. Finally, the filtrate is dried to form a superfine powder. Next, the scintillating material is mixed with a photosensitive polymer, which combines an eosin Y (tetrabromofluoroescein) used as a sensitizer dye, a co-initiator (MDEA: N-methyldiethanola-mine) and a multifunctional acrylate monomer, pentaerytritoltriacrylate (PETIA) [20]. This photosensitive formulation provides robust microstructures at the endface of an optical fiber [18, 21]. A weight ratio of 1:5.2 between the photopolymer and the scintillating powder ensures a high concentration of scintillator within the mixture. Gd_2O_2S:Eu shows excellent yield, linearity and stability upon exposure [22, 23]. This scintillator also shows sub-millisecond decay and low afterglow upon exposure at energies of the order of a few keV, thereby leading to a response time that is fast enough for numerous applications. Faster luminescence may however be achieved for instance with Gd_2O_2S:Tb material [5, 24, 25] or perovskites [9]. We verified that, upon excitation with X-rays, the residual luminescence of the photosensitive polymer is orders of magnitudes weaker than the emission from scintillators (as already evidenced in Ref. [18]).

Figure 1(a) displays a scanning electron micrograph of a resulting fiber-integrated multipixel detector. The pixel array takes the form of seven aluminum-coated scintillating micro-tips of similar geometries located on top of the seven fiber cores.

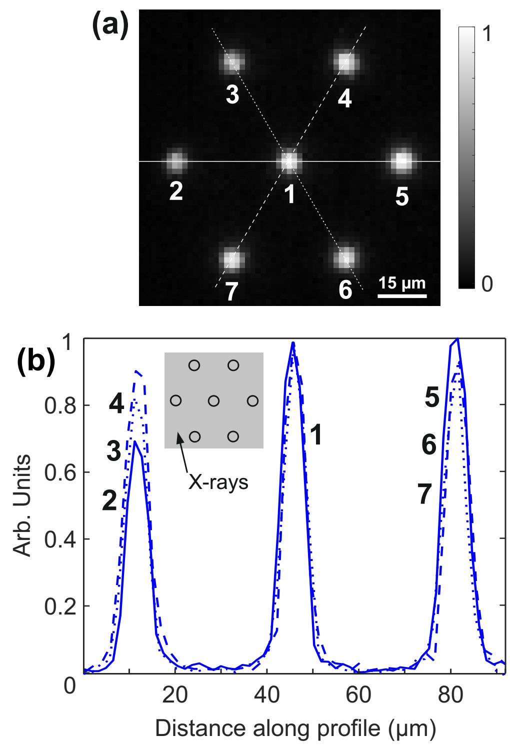

Fig. 2. (a) Optical image of the fiber output face when the pixel array is exposed to a 1x1 mm^2 radiation field (see inset of (b)). (b) Intensity plots along the three white lines of (a). Each pixel is identified with a number ranging from 1 to 7.

The microfabricated detector is demonstrated at the METROLOGIE beamline of the synchrotron SOLEIL [26]. The experimental set-up is depicted in Fig. 1(b). A monochromatic 12-keV radiation is projected onto the microstructured facet of the fiber (the beam and fiber axes are aligned). At 12 keV, a flux of 2.1 10^9 photons.s^{-1} is measured across a 1x1mm^2 radiation field. An adjustable diaphragm is positioned in front of the fiber, to control the beam width. The diaphragm and fiber detector are positioned on two independent 3D motorized stages. The bare output face of the fiber is imaged with a standard sCMOS camera (Zyla model from Andor Technology) equipped with a (x10, 0.3) microscope objective (Olympus). The camera is positioned outside the irradiation zone of the primary beam: although the optical fiber is shown straight in Fig. 1(b), it follows a S-shaped curvature in the set-up. We verified that negligible stem effect (i.e., Cerenkov effect) [27, 28] is generated by the fiber itself upon exposure: no signal is detected when a bare scintillator-free multicore fiber is placed within the above-described test-bed. The camera is used as a photometer array to simultaneously read the seven instant optical signals delivered in parallel by the fiber-integrated multipixel platform. The readout signals are obtained by integrating image intensity over 64x64-pixel regions of interest (ROI) tightly enclosing the seven output light spots (one ROI per spot). Images are recorded at a rate of 3.3 Hz.

Figure 2(a) shows an image of the output endface of the multicore fiber. The observed seven light spots originate from the scintillation light generated upon irradiation by the fiber-integrated pixel array and guided through the fiber to the camera. These light spots are well separated in the image, thereby avoiding artifactual inter-pixel crosstalk in the optical readout process. Since a relatively homogeneous distribution of light spots is imaged by the camera (see Fig. 2(b)), we conclude that the concentration of scintillators across the microtip array is almost constant and the fabrication process satisfies pixel homogeneity. Only one pixel shows a noticeably weaker optical signal. The main reason is either a lower concentration of scintillators at the tip location during photopolymerization, or a tip shape that is less efficient to outcouple light into the fiber. Regularity of the tip shape could be improved with single-mode multicore fibers (not commercialized yet). Given the few-mode nature of the fiber at the photopolymerization wavelength, the guided light used for tip fabrication shows tight intensity inhomogeneities which may affect tip shape and pixel sensitivity. Note that correction factors can be applied to the pixel array to correct signal offsets. .

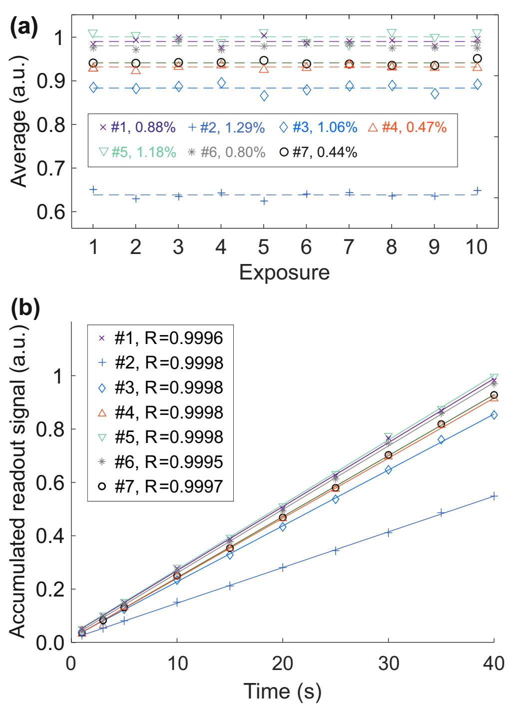

Fig. 3. (a) Repeatability of the multipixel detection system over ten successive exposures of 10s. Each point corresponds to the accumulated readout signal for each exposure. In the inset are reported the relative standard deviation to the average accumulated signal from each pixel. Pixels are identified with a number ranging from 1 and 7 (cf. Fig. 2(a)). (b) Linearity of the detector versus exposure duration (i.e., accumulated dose).

The response of our fiber-integrated multipixel detector in terms of dose linearity and repeatability is reported in Fig. 3. The measurement repeatability (Fig. 3(a)) is determined over ten exposures of ten seconds each. For the ten exposures at a near-constant radiation flux, the light intensities accumulated by each detection pixel show standard deviation from signal average spanning from 0.4 % to 1.29 %. Note that these errors are mainly due to slight variations of the X-ray intensity at the synchrotron beamline. The X-ray flux in a synchrotron is known to be a decaying function of time due to lifetime limitations of the electrons within the storage ring. To overcome this problem, electrons are periodically injected into the storage ring to compensate beam losses and keep a constant photon flux at beamlines (cf. "top-up" operation). Since our measurements are realized between two successive "top-ups", we numerically compensated the X-ray intensity decay in our data acquisition from a linear regression calculation. A linear regression being a first approximation of the real time-varying decay of the X-ray beam, residual intensity fluctuations are preserved and explain the harmonic fluctuations of the data points visible in Fig. 3(a)). Therefore the offsets to the perfect repeatability imputed to our detection system are smaller than the values given in the figure inset. The linearity of the detector with regards to the deposited dose is assessed by accumulating the signals detected by each of its fiber-integrated pixels over 1, 3, 5, 10, 15, 20, 25, 30, 35 and 40 seconds of irradiation at a near-constant flux (see Fig. 3(b)). The linearity factor R across the pixel array exceeds 0.999. Note that we did not observe noticeable performance degradation of our probe during our few-hour probe tests. We also verified detection stability with a single pixel fiber probe (implemented onto a multimode single mode fiber) during a 72h continuous exposure at the METROLOGY beamline.

To evidence potential spurious inter-pixel cross-talk in the overall detection process, the X-ray radiation is narrowed until exposing a single pixel. To this end, the diaphragm diameter is decreased down to 35 μm and the resulting pinhole is centered with respect to one of the seven pixels of the fiber probes. Fig. 4(a) reports an optical image of the output endface of the fiber when the tight X-ray pencil selectively irradiates the pixel at the center of the detection array. We see that only the exposed pixel delivers light to the camera via the multicore fiber, the neighboring detection channels remain unexcited. This is confirmed on the intensity plots of Fig. 4(b). Outside the fiber core coupled to the pixel under exposure, the detected intensity does not exceed the dark current of the camera: inter-pixel cross-talk is therefore negligible.

Our fiber detector has also been tested with the radiation from a Cu-target source (40 kV, 40 mA / Bruker D8 DISCOVER diffractometer). Figure 5 shows time traces simultaneously delivered by the seven pixels of the fiber probe upon exposure. At the beginning and at the end of the acquisition, the source shutter is closed to verify that no spurious residual light (such as in-fiber coupled room light or scintillator afterglow) is detected by the system. We see that without X-rays, the afterglow generally observed with Eu-doped gadolinium oxysulfide [22] is here negligible. When the shutter is open (during 110 seconds), seven signals are simultaneously detected with a signal-to-noise ratio ranging from 30 to 42. We measure a rise and fall times of our detection system limited by the detection rate of our camera. The shorter temporal response of the system is defined to the order of 1 ms by the decay time of the scintillators [29]. Note that the signal-to-noise ratio can be enhanced by finding an optimum combination between tip shape and scintillator concentration within the photopolymer. After metal deposition onto the tips, the pixel sensitivity is enhanced by a factor of about two.

To conclude, we introduce the concept of a multi-pixel X-ray

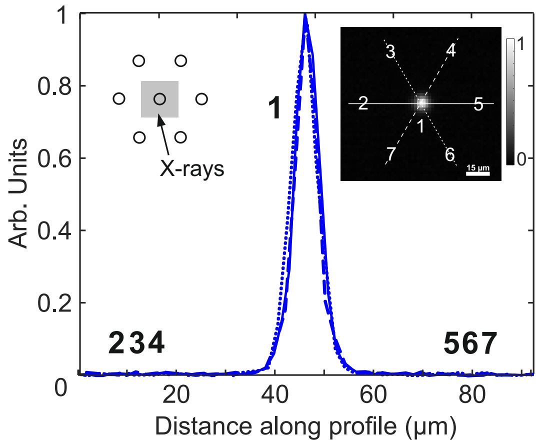

Fig. 4. Detector response when the pixel array is exposed to a 35x35 μm^2 radiation field centered with respect to the center pixel (see inset, left part). Intensity profiles are plotted along the three white lines of the top right inset which shows the optical image of the fiber output face.

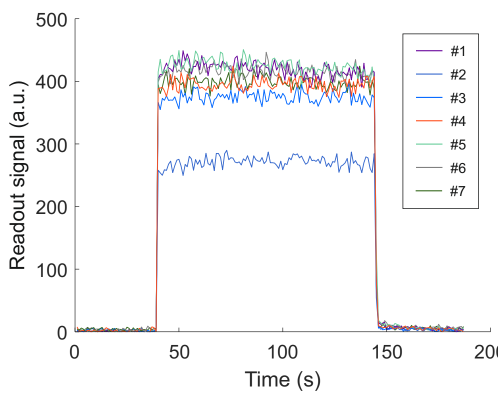

Fig. 5. Readout signal from the seven detection pixels upon a 110 s exposure to X-rays from a Cu-target source. The source shutter is closed during the first and last 40 s of the acquisition.

detector integrated at one endface of an individual multicore fiber. A seven-pixel array is demonstrated onto a narrow 125-μm diameter seven-core fiber, each pixel being engineered simultaneously on top of each fiber core by photolithography. The resulting imaging system shows good repeatability and linearity regarding the accumulated radiation dose and it is totally free from inter-pixel crosstalk. Our fiber detector could be used to perform multi-point analysis of X-ray microbeams [30]. This multipoint detection unit could also be seen as the building block of a future ultracompact camera engineered from a bundle of multicore fibers. Note that our multipixel detection architecture can be engineered with a wide variety of scintillators, including halide perovskites of high potential for X-ray detection [9]. Being compact and flexible, such fibered camera systems would enable *in situ* or *in vivo* high resolution X-ray imaging in hard-to-reach locations. By leveraging the ubiquity of fiber-optics technology, this may represent new prospects in a broad range of scientific, medical, and industrial applications.

Funding.

Acknowledgments. The authors are indebted to the METROLOGIE beamline team for its support and the allowed beam-time for our detector demonstration. This study is also partly supported by the French RENATECH network and its FEMTO-ST technological facility.

Disclosures. The authors declare no conflicts of interest.

Data availability. Data underlying the results presented in this paper are not publicly available at this time but may be obtained from the authors upon reasonable request.

REFERENCES

1. L. Beaulieu and S. Beddar, Phys. Med. & Biol. **61**, R305 (2016).
2. L. Ding, Q. Wu, Q. Wang, Y. Li, R. M. Perks, and L. Zhao, EJNMMI physics **7**, 1 (2020).
3. M. Jia, J. Wen, X. Pan, Z. Xin, F. Pang, L. He, and T. Wang, Opt. Express **29**, 1210 (2021).
4. K. Chen, J. Ren, C. Zhao, F. Liao, D. Yuan, L. Lei, and Y. Zhao, Opt. Express **29**, 22578 (2021).
5. M. Gonod, C. C. Avila, M. A. Suarez, J. Crouzilles, S. Laskri, J.-F. Vinchant, L. Aubignac, and T. Grosjean, Phys. Med. Biol. **66**, 115016 (2021).
6. A. Förster, S. Brandstetter, and C. Schulze-Briese, Phil. Trans. R. Soc. A **377**, 20180241 (2019).
7. T. Shimaoka, S. Koizumi, JH, and Kaneko, Funct. Diam. **1**, 205 (2022).
8. Y. Su, W. Ma, and Y. M. Yang, J. Semicond. **41**, 051204 (2020).
9. F. Zhou, Z. Li, W. Lan, Q. Wang, L. Ding, and Z. Jin, Small Methods **4**, 2000506 (2020).
10. L. Cartwright, N. Suchowerska, Y. Yin, J. Lambert, M. Haque, and D. McKenzie, Med. Phys. **37**, 2247 (2010).
11. H. M. Linares Rosales, L. Archambault, S. Beddar, and L. Beaulieu, Med. Phys. **47**, 4477 (2020).
12. Z. Zhao, Y. Dang, and M. Tang, "Advances in multicore fiber grating sensors," in *Photonics,* , vol. 9 (MDPI, 2022), p. 381.
13. Z. Zhao, M. Tang, and C. Lu, Opto-Electronic Adv. **3**, 190024 (2020).
14. M. Pisco and A. Cusano, Sensors **20**, 4705 (2020).
15. Y. Xiong and F. Xu, Adv. Photonics **2**, 064001 (2020).
16. Y. Xiong, H. Xu, Y. Wang, C. Wu, Z. Ding, M. Chen, Y. Hao, Y. Chen, and F. Xu, ACS Photonics **9**, 1808 (2022).
17. Y. Xiong, Y. Wang, R. Zhu, H. Xu, C. Wu, J. Chen, Y. Ma, Y. Liu, Y. Chen, K. Watanabe *et al.*, Sci. Adv. **8**, eabo0375 (2022).
18. Z. Xie, H. Maradj, M.-A. Suarez, L. Viau, V. Moutarlier, C. Filiatre, C. Fauquet, D. Tonneau, and T. Grosjean, Opt. Lett. **42**, 1361 (2017).
19. I. Dika, F. Diot, V. Bardinal, J.-p. Malval, C. Ecoffet, A. Bruyant, D. Barat, B. Reig, J.-b. Doucet, T. Camps *et al.*, J. Polym. Sci. **58**, 1796 (2020).
20. C. Ecoffet, A. Espanet, and D. Lougnot, Adv. Mater **10**, 411 (1998).
21. R. Bachelot, C. Ecoffet, D. Deloeil, P. Royer, and D.-J. Lougnot, Appl. Opt. **40**, 5860 (2001).
22. B. Ortega-Berlanga, L. Betancourt-Mendiola, C. del Angel-Olarte, L. Hernández-Adame, S. Rosales-Mendoza, and G. Palestino, Crystals **11** (2021).
23. M. A. Suarez, T. Lim, L. Robillot, V. Maillot, T. Lihoreau, P. Bontemps, L. Pazart, and T. Grosjean, Opt. Express **27**, 35588 (2019).
24. Y. Hu, Z. Qin, Y. Ma, W. Zhao, W. Sun, D. Zhang, Z. Chen, B. Wang, H. Tian, and E. Lewis, Sens. Actuator A-Phys. **269**, 188 (2018).
25. Z.Qin, Y.Hu, Y. Ma, W. Zhao, W. Sun, D. Zhang, Z. Chen, and E. Lewis, Opt. Express **24**, 5172 (2016).
26. M. Idir, P. Mercere, T. Moreno, and A. Delmotte, Synchrotron Radiat. News **19**, 18 (2006).
27. B. Lee, K. W. Jang, D. H. Cho, W. J. Yoo, G.-R. Tack, S.-C. Chung, S. Kim, and H. Cho, Nucl. Instrum. Meth. A **579**, 344 (2007).
28. S. Law, N. Suchowerska, D. McKenzie, S. Fleming, and T. Lin, Opt. Lett. **32**, 1205 (2007).
29. H. Chen, M. M. Rogalski, and J. N. Anker, Phys. Chem. Chem. Phys. **14**, 13469 (2012).
30. G. E. Ice, J. D. Budai, and J. W. Pang, Science **334**, 1234 (2011).

REFERENCES

1. L. Beaulieu and S. Beddar, “Review of plastic and liquid scintillation dosimetry for photon, electron, and proton therapy,” Phys. Med. & Biol. **61**, R305 (2016).
2. L. Ding, Q. Wu, Q. Wang, Y. Li, R. M. Perks, and L. Zhao, “Advances on inorganic scintillator-based optic fiber dosimeters,” EJNMMI physics **7**, 1–23 (2020).
3. M. Jia, J. Wen, X. Pan, Z. Xin, F. Pang, L. He, and T. Wang, “Tapered fiber radiation sensor based on ce/tb: Yag crystals for remote γ-ray dosimetry,” Opt. Express **29**, 1210–1220 (2021).
4. K. Chen, J. Ren, C. Zhao, F. Liao, D. Yuan, L. Lei, and Y. Zhao, “High-sensitivity fiber-optic x-ray detectors employing gadolinium oxysulfide composites,” Opt. Express **29**, 22578–22592 (2021).
5. M. Gonod, C. C. Avila, M. A. Suarez, J. Crouzilles, S. Laskri, J.-F. Vinchant, L. Aubignac, and T. Grosjean, “Miniaturized scintillator dosimeter for small field radiation therapy,” Phys. Med. Biol. **66**, 115016 (2021).
6. A. Förster, S. Brandstetter, and C. Schulze-Briese, “Transforming x-ray detection with hybrid photon counting detectors,” Phil. Trans. R. Soc. A **377**, 20180241 (2019).
7. T. Shimaoka, S. Koizumi, JH, and Kaneko, “Recent progress in diamond radiation detectors,” Funct. Diam. **1**, 205–220 (2022).
8. Y. Su, W. Ma, and Y. M. Yang, “Perovskite semiconductors for direct x-ray detection and imaging,” J. Semicond. **41**, 051204 (2020).
9. F. Zhou, Z. Li, W. Lan, Q. Wang, L. Ding, and Z. Jin, “Halide perovskite, a potential scintillator for x-ray detection,” Small Methods **4**, 2000506 (2020).
10. L. Cartwright, N. Suchowerska, Y. Yin, J. Lambert, M. Haque, and D. McKenzie, “Dose mapping of the rectal wall during brachytherapy with an array of scintillation dosimeters,” Med. Phys. **37**, 2247–2255 (2010).
11. H. M. Linares Rosales, L. Archambault, S. Beddar, and L. Beaulieu, “Dosimetric performance of a multipoint plastic scintillator dosimeter as a tool for real-time source tracking in high dose rate ir brachytherapy,” Med. Phys. **47**, 4477–4490 (2020).
12. Z. Zhao, Y. Dang, and M. Tang, “Advances in multicore fiber grating sensors,” in *Photonics,* vol. 9 (MDPI, 2022), p. 381.
13. Z. Zhao, M. Tang, and C. Lu, “Distributed multicore fiber sensors,” Opto-Electronic Adv. **3**, 190024–1 (2020).
14. M. Pisco and A. Cusano, “Lab-on-fiber technology: a roadmap toward multifunctional plug and play platforms,” Sensors **20**, 4705 (2020).
15. Y. Xiong and F. Xu, “Multifunctional integration on optical fiber tips: challenges and opportunities,” Adv. Photonics **2**, 064001 (2020).
16. Y. Xiong, H. Xu, Y. Wang, C. Wu, Z. Ding, M. Chen, Y. Hao, Y. Chen, and F. Xu, “Ultracompact multicore fiber de-multiplexer using an endface-integrating graphene photodetector array,” ACS Photonics **9**, 1808–1813 (2022).
17. Y. Xiong, Y. Wang, R. Zhu, H. Xu, C. Wu, J. Chen, Y. Ma, Y. Liu, Y. Chen, K. Watanabe *et al.*, “Twisted black phosphorus–based van der waals stacks for fiber-integrated polarimeters,” Sci. Adv. **8**, eabo0375 (2022).
18. Z. Xie, H. Maradj, M.-A. Suarez, L. Viau, V. Moutarlier, C. Filiatre, C. Fauquet, D. Tonneau, and T. Grosjean, “Ultracompact x-ray dosimeter based on scintillators coupled to a nano-optical antenna,” Opt. Lett. **42**, 1361–1364 (2017).
19. I. Dika, F. Diot, V. Bardinal, J.-p. Malval, C. Ecoffet, A. Bruyant, D. Barat, B. Reig, J.-b. Doucet, T. Camps *et al.*, “Near infrared photopolymer for micro-optics applications,” J. Polym. Sci. **58**, 1796–1809 (2020).
20. C. Ecoffet, A. Espanet, and D. Lougnot, “Photopolymerization by evanescent waves: A new method to obtain nanoparts,” Adv. Mater **10**, 411–414 (1998).
21. R. Bachelot, C. Ecoffet, D. Deloeil, P. Royer, and D.-J. Lougnot, “Integration of micrometer-sized polymer elements at the end of optical fibers by free-radical photopolymerization,” Appl. Opt. **40**, 5860–5871 (2001).
22. B. Ortega-Berlanga, L. Betancourt-Mendiola, C. del Angel-Olarte, L. Hernández-Adame, S. Rosales-Mendoza, and G. Palestino, “An overview of gadolinium-based oxide and oxysulfide particles: Synthesis, properties, and biomedical applications,” Crystals **11** (2021).
23. M. A. Suarez, T. Lim, L. Robillot, V. Maillot, T. Lihoreau, P. Bontemps, L. Pazart, and T. Grosjean, “Miniaturized fiber dosimeter of medical ionizing radiations on a narrow optical fiber,” Opt. Express **27**, 35588–35599 (2019).
24. Y. Hu, Z. Qin, Y. Ma, W. Zhao, W. Sun, D. Zhang, Z. Chen, B. Wang, H. Tian, and E. Lewis, “Characterization of fiber radiation dosimeters with different embedded scintillator materials for radiotherapy applications,” Sens. Actuator A-Phys. **269**, 188–195 (2018).
25. Z.Qin, Y.Hu, Y. Ma, W. Zhao, W. Sun, D. Zhang, Z. Chen, and E. Lewis, “Embedded structure fiber-optic radiation dosimeter for radiotherapy applications,” Opt. Express **24**, 5172–5185 (2016).
26. M. Idir, P. Mercere, T. Moreno, and A. Delmotte, “Technical report: Metrology and test beamline at soleil,” Synchrotron Radiat. News **19**, 18–23 (2006).
27. B. Lee, K. W. Jang, D. H. Cho, W. J. Yoo, G.-R. Tack, S.-C. Chung, S. Kim, and H. Cho, “Measurements and elimination of cherenkov light in fiber-optic scintillating detector for electron beam therapy dosimetry,” Nucl. Instrum. Meth. A **579**, 344–348 (2007).
28. S. Law, N. Suchowerska, D. McKenzie, S. Fleming, and T. Lin, “Transmission of čerenkov radiation in optical fibers,” Opt. Lett. **32**, 1205–1207 (2007).
29. H. Chen, M. M. Rogalski, and J. N. Anker, “Advances in functional x-ray imaging techniques and contrast agents,” Phys. Chem. Chem. Phys. **14**, 13469–13486 (2012).
30. G. E. Ice, J. D. Budai, and J. W. Pang, “The race to x-ray microbeam and nanobeam science,” Science **334**, 1234–1239 (2011).